

A New Compact Planar Antenna for Switching between UWB, Narrow Band and UWB with Tunable-notch Behaviors for UWB and WLAN Applications

Mansour NejatiJahromi^{1,4}, Mahdi NagshvarianJahromi², and MuhibUr Rahman³

¹Department of Electrical Engineering, Islamic Azad University, South Tehran Branch, Tehran, Iran
m_nejati@azad.ac.ir

²Department of Electrical and Computer Engineering, McMaster University, Hamilton ON, L8S 4L8, Canada
naghshvm@mcmaster.ca

³Division of Electronics and Electrical Engineering, Dongguk University, Seoul, 04620, Republic of Korea
muhib@dongguk.edu, muhib95@gmail.com

⁴Electrical and Electronic Engineering Department, Shahid sattari Aeronautical University of Science, Tehran, Iran
m_nejati@azad.ac.ir

Abstract — This paper presents continuously switchable behavior between narrowband (5.5 GHz WLAN), wideband (3-11 GHz UWB), and band-notched UWB using a miniaturized novel resonator. Three essential responses can be achieved from the same resonator by adequately utilizing the two capacitors. The first essential narrowband behavior is obtained from the resonator at 0.1pF is WLAN (5.5 GHz) operating frequency band. The second wideband behavior is achieved from the resonator to work between 3-11 GHz UWB frequency band. This behavior is achieved by changing the value of capacitors from 0.1 pF to 0.8pF. Finally, band-notched UWB response has been achieved by adjusting the position of capacitors, and this band-notch behavior can also be tuned continuously between WLAN and WiMAX frequency band. The antenna designed for these objectives have a compact size of 24×30.5 mm² including the particular ground plane. The clean and consistent radiation pattern of the antenna is observed because of the placement of the resonators in the partial ground plane. The antenna is also fabricated, and its response to three behaviors is measured for validation.

Index Terms — Band-notched UWB behavior, continuously switchable behavior, narrow-band behavior, tunable band-notched response, wide-band behavior.

I. INTRODUCTION

The wireless communication systems are highly developed in recent years, and the spectrum congestion has been highly increased. Narrow-band to wide-band switchable antennas is one of the best solutions to utilize the spectrum properly. These antennas will properly

sense the environment in the particular state and will occupy the existing frequency band instantaneously using the dynamic spectrum allocations. Secondly, the antennas and filters should be integrated so that it can reduce the overall size of the transceiver and improve the capability of antennas as an antenna filter. In this context, a new concept termed as filtering antenna that can realize the filtering functionality and radiation characteristics simultaneously is presented in past years [1-2]. This technique avoids the designing of bandpass filter and antenna separately, and thus a more compact structure can be developed which in turn profoundly improves the performance of RF front-end. By combining the benefits of above two techniques, (switchable antennas and filtering antennas), a narrowband-to-wideband continuously switchable filtering antenna could be developed.

In last decades, many research papers have been published on reconfigurable antennas and narrowband reconfigurable antennas [3-6]. A frequency tunable antenna has been proposed in [7]. The tunability in narrow frequency band has been achieved by utilizing a reconfigurable filter, while PIN diode is used to switch the behavior of antenna between wideband and narrowband. A switchable bowtie dipole antenna between narrowband and wideband response is realized in [8], by controlling the PIN diodes states. Similarly, in [9-11] different MEMS switches, varactor diodes, and PIN diodes have been implemented to achieve the switching functionality between the narrowband and wideband behavior.

Another critical and critical concern of wireless communication appliances is the miniaturization and integration methods that can reduce the overall size of

the transceiver. In this regard, several techniques of the filters and antennas integration have been proposed in the literature [12-13]. A novel antenna is achieved in [14] with filtering behavior and dual-band response while in [15] a reconfigurable slot has been used to place filtering behavior in the antenna.

Based on the research work discussed above, switchable behavior between narrowband and wideband is achieved with straightforward structure and novel resonator. This manuscript is novel in the following aspects.

(1) For wireless communication devices such as smartphones and handset mobile internet devices to access the wireless spectrum of UWB and WLAN, a continuously switchable antenna is developed as it can instantaneously occupy the available range.

(2) The UWB response is also made band-notched in the WLAN frequency band due to unavoidable electromagnetic interferences.

(3) The band-notched response is also made continuously switchable and can be shifted to WiMAX frequency band depending on the desired application.

(4) Three different behaviors are achieved from the same resonator based on capacitors placement.

(5) The designed filtering antenna is not only valid to the narrow and wideband operation but can also accomplish miniaturization in RF front-end.

In this paper, we have presented a continuously switchable behavior between narrowband (5.5 GHz WLAN), wideband (3-11 GHz UWB), and band-notched UWB using a miniaturized novel resonator. Three essential behaviors are achieved from a single antenna by adequately utilizing the two capacitors. The first important behavior is achieved from the antenna at 0.1pF is WLAN (5.5 GHz) operating frequency band. The second behavior is developed by changing the value of both capacitors to 0.8pF to operate at wideband (UWB). Finally, band-notched UWB response is achieved by further adjusting the capacitor value, and this band-notch is also made continuously tunable between WLAN and WiMAX frequency band. The antenna has a compact size, and its dimensions are $24 \times 30.5 \text{ mm}^2$. The clean and consistent radiation pattern of the antenna is also observed because of the placement of the resonators in the partial ground plane. The antenna is also fabricated, and its three behaviors response is measured.

The arrangement of the paper is carried out in the following manner. Section II contains discussion on simulation and measurement of three essential behaviors that have been achieved from the designed antenna. Section III dealt with the analysis of the resonator implemented and showed how these three behaviors could be achieved from a single resonator. Section IV deals with measurement discrepancies which are followed by conclusion in Section V.

II. DISCUSSION ON SIMULATION AND MEASUREMENTS FOR ACHIEVING THREE IMPORTANT BEHAVIORS FROM RESONATOR

A. Narrowband behavior antenna

The configuration and geometry of the narrowband antenna are shown in Fig. 1. This antenna is fabricated on Rogers RO4003 substrate with a thickness of 1.5 mm and the relative dielectric constant of $\epsilon_r=3.38$ which has a dimension of $24 \times 30.5 \text{ mm}^2$ (i.e., $W_{\text{sub}} \times L_{\text{sub}}$). The parameters of the proposed antenna are mentioned in Table 1. Two symmetrical capacitors are placed at the junction of the feedline and proposed resonators to control the response of the antenna. At 0.1pF the antenna is the good narrowband radiator and operate at 5.5 GHz WLAN frequency band.

The behavior of the antenna has been studied and simulated in Ansoft HFSS while it has been validated in CST Microwave studio suite. When the value of both capacitors are 0.1pF, then the resonator is coupled to the feedline and generates a narrowband behavior as shown in Fig. 3. The antenna is also fabricated as shown in Fig. 2 and its response at 0.1pF is correlated with the simulated one in Fig. 3.

Table 1: Dimensions (in millimeters) of the proposed antenna

Parameters	L_{sub}	W_{sub}	L_1	L_2	L_3	L_4
Value (mm)	30.5	24	13	5	1.7	1.2
Parameters	L_5	W_1	W_2	W_3	W_4	W_5
Value (mm)	0.96	22	10.6	5	2.3	0.2
Parameters	G_1	G_2	G_3	T	H	R
Value (mm)	0.2	0.25	0.2	0.017	1.5	11

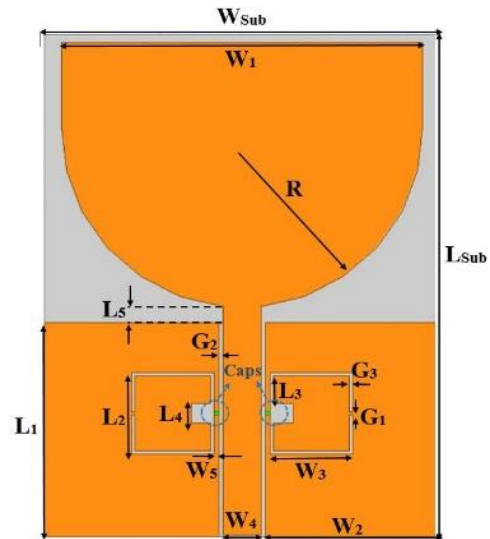


Fig. 1. Geometrical parameters of the narrowband-to-wideband antenna.



Fig. 2. Fabricated picture of the narrowband antenna.

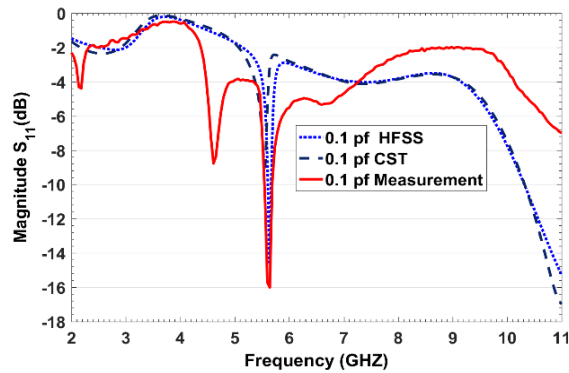


Fig. 3. Simulated and measured narrowband behavior of the antenna.

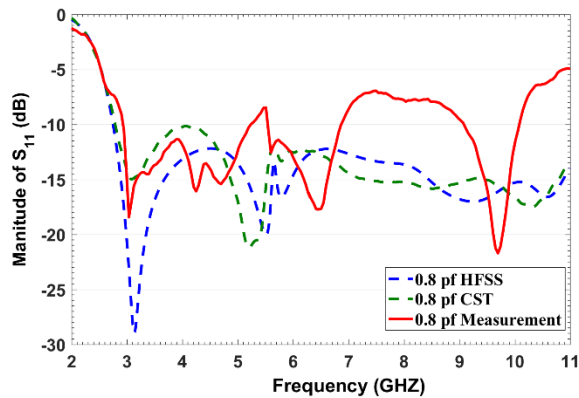


Fig. 4. Simulated and measured the wideband behavior of the antenna.

B. Wideband behavior antenna

The antenna response has been switched to wideband by changing the value of both capacitors. At 0.8pF the antenna is a good UWB radiator and operate within 3-11 GHz. The antenna at 0.8pF is also simulated and measured, and the response has been shown in Fig. 4. Also, the measurement results in comparison to numerical simulation results are shown in Fig. 5 for 0.1 PF and 0.8 PF. When the value of both capacitors are 0.8pF, then all the electromagnetic energy is transformed

to the patch radiator, and it acts as a wideband UWB antenna. This behavior can be more clearly studied in Fig. 6 where the parametric analysis has been performed, and it is shown that by increasing the capacitor value, the response has been shifting from narrowband-to-wideband. The measured switching behavior is also more clearly elaborated in Fig. 6. In this way, we can switch the antenna behavior between narrowband-to-wideband behaviors with straightforward structure and analysis.

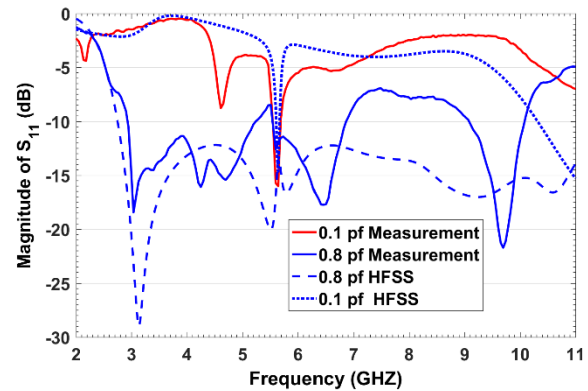


Fig. 5. The transformation from narrowband-to-wideband behavior.

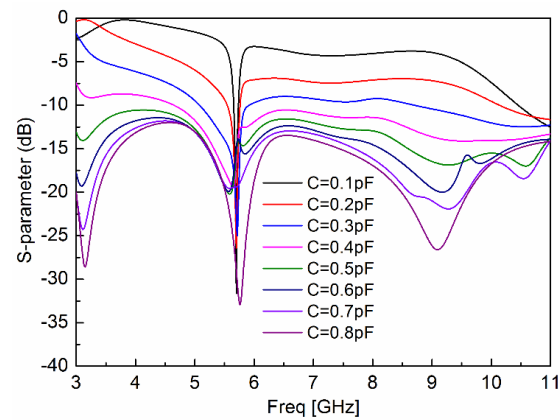


Fig. 6. Parametric analysis between narrowband and wideband behavior by varying capacitor.

C. Continuously tunable band-notched behavior antenna

By shifting both capacitors from the resonator-feed line junction to resonator internally, there is no more narrowband behavior as all electromagnetic energy will be radiated from the patch. Both capacitors have been shifted to the resonator internally as shown in Fig. 7. Now this resonator will act as a filter resonator and can be controlled by using the value of both capacitors. The overall response of the antenna will be wideband having continuously switchable notched band between WLAN

and WiMAX which causes unavoidable interference within UWB frequency band. In this way, we have achieved three important behaviors from the single resonator, which make it advantageous over other reported resonators and antennas.

It can be seen from Fig. 8 that WLAN band-notched UWB antenna response is achieved at 0.1pF while WiMAX band-notched UWB antenna is developed utilizing 0.6pF capacitor. In this way, the response can be made continuously switchable between the two interfering bands depending upon the application. It is due to the reason that the effective resonator length corresponds to the fundamental resonance frequency of 5.3 GHz. This resonance frequency can be further changed by varying the capacitors.

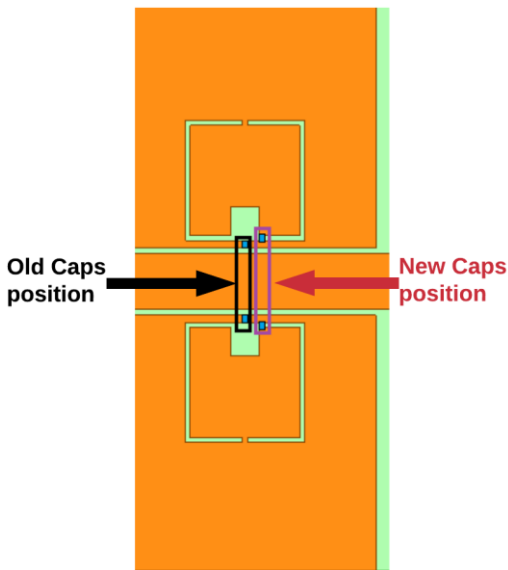


Fig. 7. Changing the position of capacitors for achieving continuously switchable band-notched UWB behavior.

The measurement of the band-notched UWB antenna developed are also carried out at 0.1pF and 0.5pF, and it is seen that the notch band is switching continuously. Figure 9 shows that there is band notch at 5.1 GHz due to the resonance of the resonator. This notched band has been made switchable, and at 0.5pF it is shifted towards 3.5 GHz WiMAX frequency band. The comparison between simulated and measured response at 0.5pf is shown in Fig. 10. The discrepancy between the simulated and measured responses is because of nonperfect cutting of the substrate edges while soldering the SMA connector.

The normalized radiation pattern of wide-band UWB antenna at 0.8pf is also shown in Fig. 11. Because of placing resonators at the ground plane, consistent radiation patterns are obtained for the antenna. The antenna worked in UWB mode and the radiation pattern display dipole type radiation. The primary purpose the radiation pattern is to demonstrate that the antenna

radiates over the full frequency bandwidth. The peak antenna gain (dB) in CST and HFSS for the wide-band antenna has been shown in Fig. 12. The gain is very stable in the overall frequency band of 3-11 GHz.

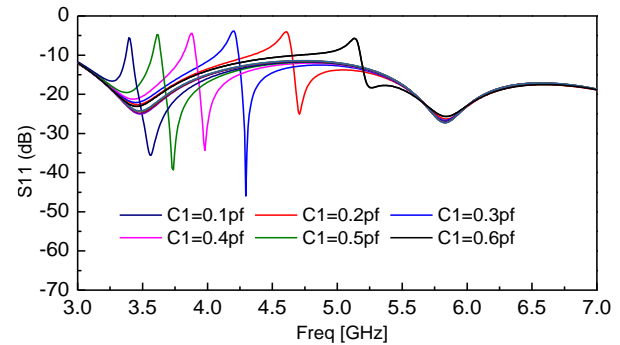


Fig. 8. Switching of notched-band between WLAN and WiMAX frequency band by changing capacitors value.

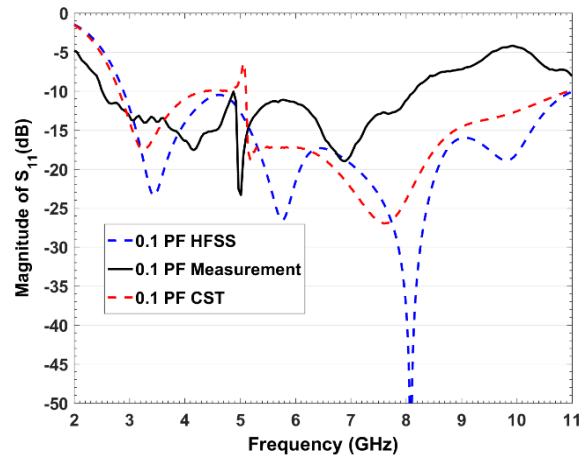


Fig. 9. Simulation and measurement of switchable band-notched UWB antenna at 0.1pF.

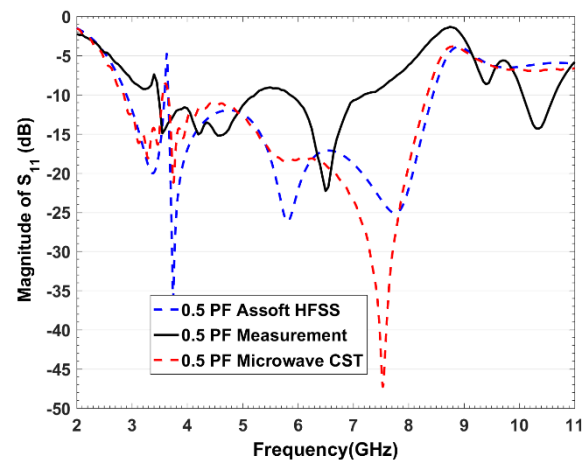


Fig. 10. Simulation and measurement of switchable band-notched UWB antenna at 0.8pF.

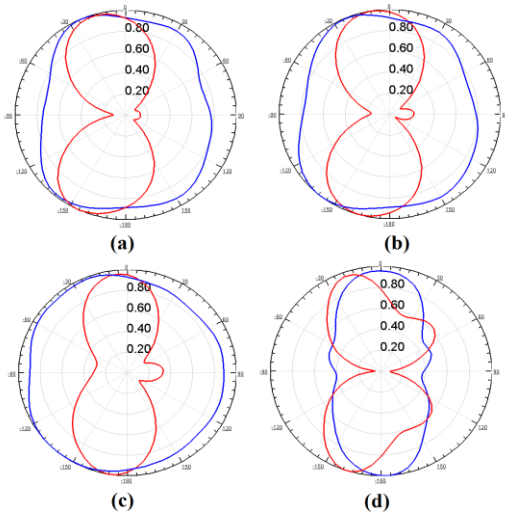


Fig. 11. Radiation patterns of switchable wide-band UWB antenna at 0.8pF: (a) 3.4 GHz, (b) 4.8 GHz, (c) 5.9 GHz, (d) 8.2 GHz. Red lines (E-plane) and blue lines (H-plane).

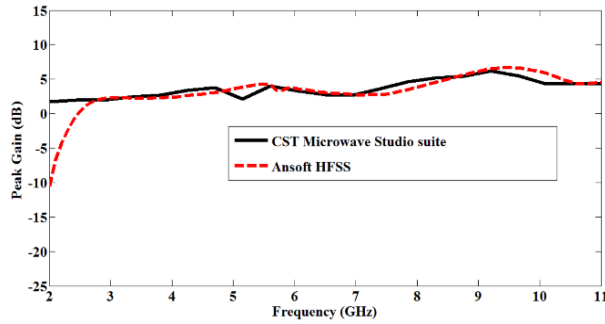


Fig. 12. Peak antenna gain for the wideband antenna in dB having capacitor value = 0.8pF.

III. DISCUSSION AND ANALYSIS ON SQUARE SEMI COMPLEMENTARY SPLIT RING RESONATOR (S-SCSRR)

The proposed miniaturized resonator is shown in Fig. 13 while its dimensions are listed in Table 1. The analysis of the resonator and its corresponding start and stop frequencies are calculated which validates our experimental results. It is proved that the homogeneous media with effective permeability (μ_{eff}) and effective permittivity (ϵ_{eff}) can replace the effective medium theory of inhomogeneous left-handed media. In such case, it should be noted that the wavelength is large enough in comparison with the basic scattering element dimensions. In such scenario, properties of non-homogeneous media become equivalent to that of homogeneous media. Thus, the condition developed that the average cell size must be less than a quarter wavelength, $l = \lambda/4$, and this condition guarantees that the wave will propagate inside a metamaterial media and the unit cell will act as a lumped portion of a circuit.

The μ_{eff} and ϵ_{eff} can be calculated from the following equations [16-19]:

$$\Gamma = k \pm \sqrt{K^2 - 1}. \quad (1)$$

Where, the sign of \pm is determined from the condition of $|\Gamma| \leq 1$:

$$k = \frac{S_{11}^2 - S_{21}^2 + 1}{2S_{11}}$$

$$Z_{\text{eff}} = \sqrt{\frac{\mu_{\text{eff}}}{\epsilon_{\text{eff}}}} = \left(\frac{1 + \Gamma}{1 - \Gamma} \right) \frac{Z_a^{\text{TL}}}{Z_l^{\text{TL}}}, \quad (2)$$

$$n = n' - jn'' = \sqrt{\epsilon_{\text{eff}} \mu_{\text{eff}}} \\ = \pm \frac{c}{j\omega l} \cosh^{-1} \left(\frac{1 - S_{11}^2 - S_{21}^2}{2S_{21}} \right), \quad (3)$$

$$\epsilon_{\text{eff}} = \epsilon_{\text{eff}}' - j\epsilon_{\text{eff}}'' = \frac{n}{Z_{\text{eff}}}, \quad (4)$$

$$\mu_{\text{eff}} = \mu_{\text{eff}}' - j\mu_{\text{eff}}'' = n Z_{\text{eff}}, \quad (5)$$

Where, Z^{TL} and Z_a^{TL} are the characteristics impedance.

The former one is in the case of reference transmission line while the later one is the transmission line having air-filled and n represents the effective refractive index.

An S-SCSRR can engrave as a square ring in the ground plane. It is noteworthy that the proposed S-CSRR is not the dual of conventional SRR, which can be analyzed using babinet principle. Also, the effective length of the LRs is designed at $\lambda/4$ at the center frequency of the selected band that is 5.5 GHz in our analysis. These LRs dramatically reduces the size of the resonator as it is inserted in the main transmission line and thus we call it miniaturized S-SCSRR. At our desired frequency these lines couple magnetically to the S-SCSRR and thus create resonance. This resonance is advantageously used as narrow-passband in narrowband antenna while narrow-stopband in band-notched UWB antenna. The overall length of the S-SCSRR is almost $\lambda/2$ while the turn ratio (coupling coefficient can be

calculated as $n = \sqrt{\frac{Z_{\text{cpw}}}{Z_{\text{os}}}}$, where Z_{os} is the slot line

characteristics impedance, and Z_{cpw} is the CPW line characteristics impedance. The reflection (S_{11}) and transmission coefficient (S_{21}) in the analysis is determined by investigating the resonator as two port matched filter [20]. It is noteworthy that when capacitors are 0.1pF to work as an open circuit, then there is a strong coupling between two slots, which generates a narrowband response in the center frequency of 5.52 GHz calculated from Equation (7). When the capacitors values are increased to 0.7pF or 0.8pF, then the resonance frequency is dependent on the coupling between CPW and resonator. The start, center, and stop frequencies are calculated in this case using Equations (6-8), having values of 3.12 GHz, 5.52 GHz, and 9.23 GHz, respectively.

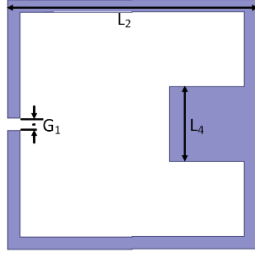


Fig. 13. Structure of the proposed novel miniaturized resonator.

The start, stop, and center frequencies of the resonator can be calculated using the following equations developed from the analysis. It is calculated from the analysis that the center frequency of the resonator lies at 5.5 GHz and so the resonator is responsible in case of narrowband behavior as well as band-notching behavior in the last scenario. In this way, the center frequency is utilized to develop narrow-band behavior as well as band-notched wide-band behavior:

$$f_{start} = \frac{\lambda_g}{4} = \frac{300}{4(3L_2 + 3L_4 - G_1)\sqrt{\epsilon_{eff}(CPW)}}, \quad (6)$$

$$= 3.12GHz$$

$$f_{center} = \frac{\lambda_g}{2} = \frac{300}{2(3L_2 + 3L_4 - G_1)\sqrt{\epsilon_{eff}(CPW)}} \sqrt{\frac{Z_{(cpw)}}{Z_{os}(f_{start})}}, \quad (7)$$

$$= 5.52GHz$$

$$f_{stop} = \lambda_g = \frac{300}{(3L_2 + 3L_4 - G_1)\sqrt{\epsilon_{eff}(CPW)}} \sqrt{\frac{Z_{(cpw)}}{Z_{os}(f_{stop})}}. \quad (8)$$

$$= 9.23GHz$$

IV. MEASUREMENT DISCREPANCIES

The measurement discrepancies have been analyzed, and it is found that it is because of non-perfect cutting of the substrate edges while soldering the SMA connector. Due to non-perfect cutting, there arises a gap between SMA and ground plane that has been highlighted in Fig. 14. This measurement discrepancy can be depicted from Fig. 9 and Fig. 10 where the measurement has been performed for achieving band-notched wideband behavior.

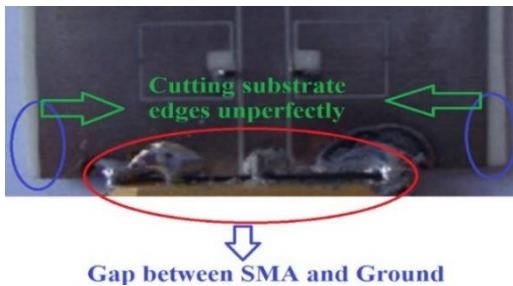


Fig. 14. Non-perfect cutting of substrate edges while soldering connector.

V. CONCLUSION

This paper presented continuously switchable behavior between narrowband (5.5 GHz WLAN), wideband (3-11 GHz UWB), and band-notched UWB using a miniaturized novel resonator. Three essential behaviors are achieved from the same resonator by adequately adjusting two capacitors. The first significant behavior produced by the antenna at 0.1pF is WLAN (5.5 GHz) operating frequency band. The second behavior from the antenna to work between 3-11 GHz UWB frequency band is achieved by changing the value of both capacitors to 0.8pF. Finally, band-notched UWB response is achieved by adjusting the position of the capacitor, and this band-notch behavior can also be tuned continuously between WLAN and WiMAX frequency band. The antenna is designed and fabricated for these behaviors and measured. Consistent radiation pattern and approximately flat antenna gain are observed because of the placement of the resonators in the partial ground plane. The antenna is also fabricated, and three different behaviors are measured using the proposed antenna for validation.

ACKNOWLEDGMENT

The authors would like to thank Islamic Azad University, South Tehran branch for their help & support sincerely.

REFERENCES

- [1] H. M. Hizan, I. C. Hunter, and A. I. Abunjaileh, "Integrated dual-band radiating bandpass filter using dual-mode circular cavities," *IEEE Microw. Wireless Compon. Lett.*, vol. 21, no. 5, pp. 246-248, May 2011.
- [2] Y. Yusuf, H. Cheng, and X. Gong, "A seamless integration of 3-D vertical filters with highly efficient slot antennas," *IEEE Trans. Antennas Propag.*, vol. 59, no. 11, pp. 4016-4022, Nov. 2011.
- [3] X. L. Yang, J. C. Lin, G. Chen, and F. L. Kong, "Frequency reconfigurable antenna for wireless communications using GaAs FET switch," *IEEE Antennas Wireless Propag. Lett.*, vol. 14, pp. 807-810, Dec. 2015.
- [4] M. Konca and P. A. Warr, "A frequency-reconfigurable antenna architecture using dielectric fluids," *IEEE Trans. Antennas Propag.*, vol. 63, no. 12, pp. 5280-5286, Dec. 2015.
- [5] S. Danesh, S. K. A. Rahim, M. Abedian, and M. R. Hamid, "A compact frequency-reconfigurable dielectric resonator antenna for LTE/WWAN and WLAN applications," *IEEE Antennas Wireless Propag. Lett.*, vol. 14, pp. 486-489, 2014.
- [6] M. Rahman "CPW fed miniaturized UWB tri-notch antenna with bandwidth enhancement," *Advances in Electrical Engineering.*, vol. 2016, pp. 1-5, 2016.

- [7] P. Y. Qin, F. Wei, and Y. J. Guo, "A wideband-to-narrowband tunable antenna using a reconfigurable filter," *IEEE Trans. Antennas Propag.*, vol. 63, no. 5, pp. 2282-2285, May 2015.
- [8] L. Ge and K.-M. Luk, "A band-reconfigurable antenna based on directed dipole," *IEEE Trans. Antennas Propag.*, vol. 62, no. 1, pp. 64-71, Jan. 2014.
- [9] A. K. Horestani, Z. Shaterian, J. Naqui, F. Martín, and C. Fumeaux, "Reconfigurable and tunable S-shaped split-ring resonators and application in band-notched UWB antennas," *IEEE Trans. Antennas Propag.*, vol. 64, no. 9, pp. 3766-3776, Sep. 2016.
- [10] H. Rajagopalan, J. M. Kovitz, and Y. Rahmat-Samii, "MEMS reconfigurable optimized E-shaped patch antenna design for cognitive radio," *IEEE Trans. Antennas Propag.*, vol. 62, no. 3, pp. 1056-1064, Mar. 2014.
- [11] T. Li, H. Zhai, L. Li, and C. Liang, "Frequency-reconfigurable bow-tie antenna with a wide tuning range," *IEEE Antennas Wireless Propag. Lett.*, vol. 13, pp. 1549-1552, Aug. 2014.
- [12] J. Shi, et al., "A compact differential filtering quasi-Yagi antenna with high-frequency selectivity and low cross-polarization levels," *IEEE Antennas Wireless Propag. Lett.*, vol. 14, pp. 1573-1576, 2015.
- [13] G.-H. Sun, S.-W. Wong, L. Zhu, and Q.-X. Chu, "A compact printed filtering antenna with good suppression of upper harmonic band," *IEEE Antennas Wireless Propag. Lett.*, vol. 15, pp. 1349-1352, Apr. 2016.
- [14] C. X. Mao, et al., "Dual-band patch antenna with filtering performance and harmonic suppression," *IEEE Trans. Antennas Propag.*, vol. 64, no. 9, pp. 4074-4077, Sep. 2016.
- [15] M. M. Fakharian, P. Rezaei, A. A. Orouji, and M. Soltanpur, "A wideband and reconfigurable filtering slot antenna," *IEEE Antennas Wireless Propag. Lett.*, vol. 15, pp. 1610-1613, 2016.
- [16] S.-G. Mao, S.-L. Chen, and C.-W. Huang, "Effective electromagnetic parameters of novel distributed left-handed microstrip lines," *IEEE Trans. Microw. Theory Tech.*, vol. 53, no. 4, pp. 1515-1521, 2005.
- [17] A. M. Nicholson and G. F. Ross, "Measurements of the intrinsic properties of materials by time-domain techniques," *IEEE Trans. Instrum. Meas.*, vol. 19, no. 4, pp. 377-382, 1970.
- [18] W. B. Weir, "Automatic measurements of complex dielectric constant and permeability at microwave frequencies," *Proc. IEEE*, vol. 62, no. 1, pp. 33-36, 1974.
- [19] M. NaghshvarianJahromi and M. Tayarani, "Defected ground structure band-stop filter by semi-complementary split ring resonators," *IET Microwaves, Antennas & Propagation*, vol. 5, no. 11, pp. 1386-1391, Aug. 19, 2011.
- [20] M. NaghshvarianJahromi and A. Ghorbani, "On the behavior of compact ultrawideband tunable bandwidth semi-complementary split ring resonator bandpass filter," *Microwave and Optical Technology Letters*, vol. 57, no. 1, pp. 256-263, 2015.



Mansour NejatiJahromi was born in 1970 in Jahrom. He received the B.S. degree in Electronic Engineering from SSA University of Science and Technology, Tehran, Iran, in 1993. He also obtained the M.S. degree in Communication from K. N. Toosi University of Technology, Tehran, Iran, in 1999, and the Ph.D. degree in Communications from Amirkabir University of Technology (AUT), Tehran, Iran, in 2008. He is an Assistant Professor in the Department of Electronic and Electrical Engineering, SSA University & Islamic Azad University, Tehran South Branch.



Mahdi Naghshvarianjahromi received M.S. degree in Communications engineering from Amirkabir University of Technology (AUT) in 2014. He is currently a Ph.D. student in Electrical and Computer Engineering at McMaster University. His current research interests are antennas, arrays, all devices throughout whole RF spectrum, fiber optic communications system and nonlinear impairment mitigation, smart home and automatic disease diagnosis, computer sciences, statistical processing and brain-like intelligence.



MuhibUr Rahman received the M.S. degree in Electrical (Telecommunication) Engineering from Military College of Signals, National University of Sciences and Technology, (NUST) Islamabad, Pakistan, in March 2016. Currently, he is a graduate Research Assistant in Electronics and Electrical Engineering at Dongguk University, Seoul, Republic of Korea. His current research interests include Narrow and Wide-band antennas, UWB band-notched antennas, MIMO UWB antennas, Microstrip bandpass and bandstop filters and metamaterial inspired structures. Rahman has published several research papers, and he is the Reviewer of PIER series, Sensors, Applied Sciences, IJMW, MOTL, and AEU.